Fracture Study of Edge Cracked Aluminium Panel Using Extended Finite Element Method

JIS TOM

A Thesis Submitted to

Indian Institute of Technology Hyderabad

In Partial Fulfillment of the Requirements for

The Degree of Master of Technology

भारतीय प्रौद्योगिकी संस्थान हैदराबाद

Indian Institute of Technology Hyderabad

Department of Mechanical and Aerospace Engineering

July 2014

Declaration

I declare that this written submission represents my ideas in my own words, and where ideas or words of others have been included, I have adequately cited and referenced the original sources. I also declare that I have adhered to all principles of academic honesty and integrity and have not misrepresented or fabricated or falsified any idea/data/fact/source in my submission. I understand that any violation of the above will be a cause for disciplinary action by the Institute and can also evoke penal action from the sources that have thus not been properly cited, or from whom proper permission has not been taken when needed.

JIS TOM

ME12M1012

Approval Sheet

This Thesis entitled "**Fracture Study of Edge Cracked Aluminium Panel Using Extended Finite Element Method**" by JIS TOM is approved for the degree of Master of Technology from IIT Hyderabad
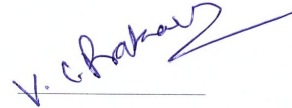
Dr. S Suriya Prakash
External Examiner
Asst. Professor, IIT Hyderabad

Dr. M Ramji
Internal Examiner
Asst. Professor, IIT Hyderabad

Dr. Viswanath Chinthapenta
Adviser
Asst. Professor, IIT Hyderabad

Dr. V C Prakash
Chairman
Asst. Professor, IIT Hyderabad

iv

Acknowledgements

Dedication

To My Late Grand Parents

Abstract

The extended finite element (XFEM) is a special kind of numerical method to handle discontinuities and singularities. Hence, it is an indispensable tool for modeling crack. In this work we are exploring the ability of XFEM for modeling the different type of fracture problems. We studied three type of fracture problems such as static crack tip fields characterization, fatigue life estimation of a cracked Al 2014-T6 panel and the crack propagation studies using XFEM.

The XFEM modeling of statically loaded crack is used to validate the least square algorithm proposed by Yoneyanama et. al. [1] for evaluating fracture parameters. In general, stress intensity factor (SIF) and T-stress are used for characterizing the stress field around the crack tip. These fracture parameters are estimated using the displacement field around the crack tip obtained experimentally through 2D digital image correlation (DIC) techniques and numerically through XFEM. It is observed that in case of parallel cracks more parameters are needed to represent the displacement field due to mixed-mode loading because of crack interactions.

In part two, the fatigue life of Al 2014-T6 panel with straight and inclined edge crack is investigated using XFEM and experiments. Fatigue tests are conducted using MTS Landmark$^\circledR$ and DIC is used to monitoring the crack tip position accurately. The life of the cracked panels are predicted numerically using ABAQUS 6.9 through XFEM. The prediction from the simulations are in reasonable agreement with the experimental prediction.

Finally, the crack propagation studies are also carried out in ABAQUS using XFEM. Conventional FEM has limitations such as necessity of re-meshing at the end of each step and crack growth path limited to inter element boundaries, etc. However, by using XFEM we overcame these limitations. And using XFEM modelling we carried out crack propagation of straight and inclined cracks. However, XFEM based crack propagation studies could not be extended to parallel cracks due to in capability of ABAQUS to model multiple cracks using XFEM.

Contents

Chapter 1

Introduction and Literature Review

1.1 Introduction

No structure is devoid of flaws. A designer has to estimate the lifetime considering the defect distribution in the structure. Especially, the load bearing structures with pre-existing flaws or stress concentrations are susceptible to fracture. Usually these structure and its components are designed to withstand stress concentrations. Further, stress concentrations can also occur from the joints of the structures like welds, rivets and fasteners. The cracks can be found due to the mechanical loading during manufacturing or because of the stresses induced during thermo-mechanical processes (such as welding or heat treatment) etc. In the cracked structures due to application of repeated loads or due to combination of loads and environmental attack, cracks grow with time. The residual strength of the structure decreases progressively with increasing crack length and eventually falls below the designed service load. From this moment, the structure is liable to failure. In order to have control over crack propagation, one need to estimate how fast crack grows and how fast residual strength decreases.

Finite element method (FEM) is widely used for fracture problems from several decades even though some numerical difficulties are present. To list a few, to represent the crack tip

singularity, remeshing with the advancing crack, crack branching and etc are the common difficulties with the Galerkin finite element methods. Mesh refinement is usually necessary near the crack tips in order to represent the asymptotic fields associated with the crack tips. And for propagating crack re-meshing is necessary. Using XFEM the above mentioned problems can be avoided.

In this work we are using XFEM for several fracture problems. Our work can be divided into three parts. In the first part, crack is modelled using XFEM to obtain the displacement field and from that SIF crack tip parameters are estimated using over-deterministic least square method [2, 1]. Further, the displacement fields obtained from FEM are validated with the DIC displacement fields. In the second part, fatigue life is estimated using experiments and predicted using XFEM simulations. In the third part, crack propagation modelling is carried out using XFEM.

The structure of this report is as follows: Chapter 1 give a brief introduction and literature review about fracture mechanics, XFEM, evaluation of fracture parameters from displacement field, fatigue life prediction using XFEM and crack propagation using XFEM Chapter 2 contain the methodology, experimental and numerical techniques for finding fracture parameters from displacement field. And using this we study the mixed mode fracture parameters for straight, inclined and parallel cracks.

In chapter 3, we carry out the experimental and numerical study of fatigue crack growth of edge cracked aluminum plate using XFEM and DIC.

In Chapter 4 we present our studies on crack propagation in aluminum panels using XFEM.

1.2 Literature Review

1.2.1 Fracture mechanics

Crack is a planar discontinuity, that is the class of defects which exhibit jump discontinuity across it and a singularity at the tip. Based on the loading the deformation field of the crack can be classified into three modes, as shown in Fig. 1.1. Mode 1 is an crack opening mode, mode 2 corresponds to in-plane shear and mode 3 is out-of plane shear. The fields

(a) Mode I (b) Mode II (c) Mode II
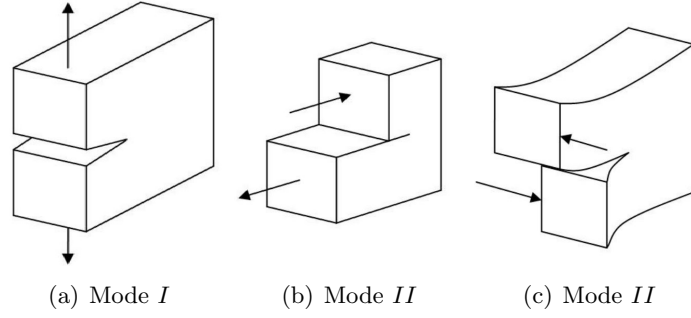
Figure 1.1: Modes of Crack
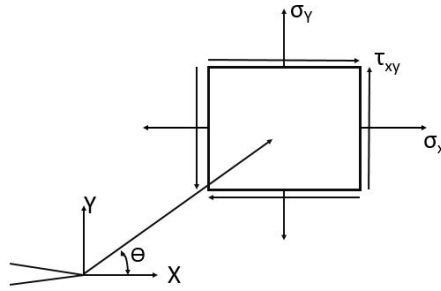
Figure 1.2: Crack tip

near the crack tip may then be characterized by the three stress intensity factors (SIF), K_I, K_{II}, and K_{III} - corresponding to the three types of loading shown in Fig. 1.1

The SIFs are related to the in-plane traction vector at a distance r ahead of the crack tip by Eq. 1.1 where r and θ are as shown in Fig. 1.2

$$(\sigma_{22} + i\tau_{12}) = \frac{K_I + iK_{II}}{\sqrt{2\pi r}} \tag{1.1}$$

The relative amount of mode II to mode I loading on a specimen is characterized by the mode angle

$$\psi = \arctan\left(\frac{K_{II}}{K_I}\right) \tag{1.2}$$

with $\psi = 0^o$ for pure mode I loading, and $\psi = 90°$ for pure mode II. The resulting Cartesian components of the displacements near the crack tip can be expressed as follows

3

$$u = \left(u_x^1\right) + \left(u_x^2\right) + \left(u_y^1\right) - \left(u_y^1\right) \tag{1.3}$$

$$u_x^1 = \frac{K_1}{2\mu}\sqrt{\frac{r}{2\pi}}\cos\left(\frac{\theta}{2}\right)\left[k - 1 + 2\sin^2\left(\frac{\theta}{2}\right)\right] \tag{1.4}$$

$$u_x^2 = \frac{K_2}{2\mu}\sqrt{\frac{r}{2\pi}}\sin\left(\frac{\theta}{2}\right)\left[k + 1 + 2\cos^2\left(\frac{\theta}{2}\right)\right] \tag{1.5}$$

$$u_y^1 = \frac{K_1}{2\mu}\sqrt{\frac{r}{2\pi}}\sin\left(\frac{\theta}{2}\right)\left[k + 1 - 2\cos^2\left(\frac{\theta}{2}\right)\right] \tag{1.6}$$

$$u_y^2 = \frac{K_1}{2\mu}\sqrt{\frac{r}{2\pi}}\cos\left(\frac{\theta}{2}\right)\left[k - 1 - 2\sin^2\left(\frac{\theta}{2}\right)\right] \tag{1.7}$$

$$k = 3 - 4\mu \tag{1.8}$$

$$\mu = \frac{E}{2\left(1 + \nu\right)} \tag{1.9}$$

where, k and μ are the Kolosov constant and shear modulus respectively.

It is evident that the above displacement fields and the corresponding stress fields are asymptotic in nature.

Another way of characterizing a crack is to use so called energy methods [3]. The energy release rate is one such method. The energy release rate often denoted by G is the amount of energy, per unit length along the crack edge, that is supplied by the elastic energy in the body and by the loading system in creating the new fracture surface area. The energy release rate is shown below in the Griffith energy balance

$$\frac{dW}{da} - \frac{dU}{da} = \frac{d\Gamma}{da} \tag{1.10}$$

where W is the external work, U is the elastic energy, Γ is the energy required for crack growth, and a is the length of the crack. When the left hand side is divided by the sample thickness, the energy release rate, G, is obtained. If $G > G_c$ then the crack will propagate, with G_c being the fracture toughness of the material. These two methods may be related to each other by

$$G = \frac{\left(K_I^2 + K_{II}^2\right)}{E} \tag{1.11}$$

4

1.2.2 Extended Finite Element Method(XFEM)

Watwood [4] in 1970's studied about use of finite element method for prediction of crack behavior. He observed that very fine mesh is needed near crack tips to represent large stress gradients. Nakamura et al. [5] studied about 3-D stress fields near the crack front and calculated approximate size of 3-D stress region. They also proposed a special kind of meshing for the crack tip in which element size gradually increased with radial distance from the crack tip. In 1995 Fernado C et al [6] studied about crack tips meshing. This extensive study on crack meshing shows that the conventional finite element method, for fracture problems is highly mesh depended and studies had been done in 90's about a mesh independent model. As a result extended finite element method is evolved as a mesh independent method which can solve many problems with modeling cracks. Bubushka et al. [7] proposed partition of unity finite element method that features the ability to include in the finite element space knowledge about the partial differential equation being solved. An additional feature of this meshless method is that finite element space of any desired regularity can be constructed very easily. Belitschko et al. [8] introduced a new technique which is later known as XFEM, for modelling cracks in the finite element framework in which standard displacement-based approximation is enriched near a crack by incorporating both discontinuous fields and the near tip asymptotic fields through a partition of unity method. This technique allows the entire crack to be represented independently of the mesh, and so remeshing is not necessary to model crack growth. Since crack contains singularity and discontinuity, XFEM can be used for modeling crack.

The basis of XFEM is that the shape functions in the finite element method exhibits the properties of partition of unity function.In the finite element method, a basis function, N_i , is associated with with a node i. n is the number of nodes in the mesh. These shape functions form a partition of unity[7]

$$\sum_{i=1}^{n} N_i\left(x\right) = 1 \tag{1.12}$$

It follows that any arbitrary function $\phi(x)$ may be reproduced exactly by

$$\sum_{i=1}^{n} N_i(x)\,\phi(x) = \phi(x) \tag{1.13}$$

It is this ability that forms the basis of the XFEM. By appropriately choosing the function $\phi(x)$ for each node, a priori knowledge of a model's behavior may be incorporated while retaining the firm mathematical basis of standard finite element analysis.

In linear elastic fracture analysis, two set of functions are used to handle the presence of a crack: a discontinuous function for the crack line and a set of asymptotic functions for the crack tip. Let the interior of the crack surface be denoted by Γ and the crack tip by Λ. The set of all nodes is N; nodes whose support is cut by the crack tip is N_Λ; and those nodes whose support is cut by the crack line are denoted by N_Γ $(N_\Gamma \cap N_\Lambda = 0)$ [9] The enriched displacement approximation then becomes [7]

$$u^h(x) = \sum_{i\epsilon n} N_i(x) \left[u_i + H(x)\,a_j + \sum_{\alpha=1}^{4} \phi_\alpha(x)\,b_k^\alpha \right] \tag{1.14}$$

where $j\epsilon N_\Gamma$, $k\epsilon N_\Lambda$, u_i is the nodal displacement vector of the continuous part of the finite element solution, a_j is the nodal enriched degree of freedom vector of the discontinuous crack line function, and b_K^α are the nodal enriched degree of freedom vectors of the asymptotic crack tip.

$$H(x) = \begin{cases} +1\,if\,(x - x^*)\,.n \\ -1\,otherwise \end{cases} \tag{1.15}$$

where x is a sample (integration) point, x^* is the projection of x onto the crack surface, and n is the unit outward normal to the crack at x^*. The asymptotic functions associated with the crack tip are

$$[\phi(X)\,,\alpha = 1 - 4] = \left[\sqrt{r}\sin\frac{\theta}{2}, \sqrt{r}\cos\frac{\theta}{2}, \sqrt{r}\sin\frac{\theta}{2}sin\theta, \sqrt{r}\cos\frac{\theta}{2}sin\theta \right] \tag{1.16}$$

Figure 1.3 shows the type of enrichment active on each node in an isotropic fracture
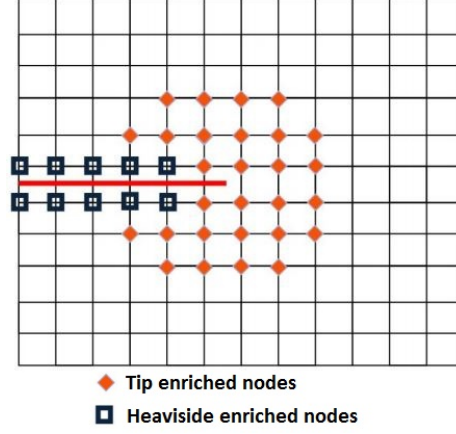
Figure 1.3: Nodal enrichment for XFEM

model

1.2.3 Fracture Parameters From Displacement Field

The presence of crack in a structure results in redistribution of displacement, stress and strain around the crack tip. In general, stress intensity factor (SIF) and T-stress are used for characterizing the stress filed around the crack tip. These are the major fracture parameters, whose knowledge is essential for understanding crack growth behavior. SIF depends on the far field stress (σ), flaw size (a), component geometry and the mode of loading [10].

$$\sigma_{ij} = \frac{K}{2\pi r} f_{ij}(\theta) \tag{1.17}$$

Where, K = stress intensity factor

The SIFs can be evaluated analytically, numerically and experimentally. Most of the analytical solutions are based on highly idealized models of the component geometry. They only provide the basic relations to find out the fracture parameters. Analytical closed-form solutions are available for various simple configurations in SIF data hand book [11]. But analytical techniques are arduous and feasible only for simple geometries. For complex configurations, SIF is extracted from experimental or numerical analysis.

Rice et al [12] correlated small crack tip plastic zones in terms of the elastic stress intensity factor and T-stress. T-stress is a non-singular stress term which acts parallel to

the crack plane. By investigating crack in homogeneous materials under a mode I load, Cotterell et al [13] concluded that the T-stress plays an important role in the directional stability of the crack propagation. The crack is directionally stable if the T-stress is negative and unstable if it is positive.

Many mathematical models have proposed to represent displacement fields around the crack tip. Some of them are a series type of equations with several fracture parameters as coefficients. K Ramesh et al [14] brought out equivalence of various multi-parameter equations such as generalized Westergaard, William's eigen function expansion and Atluri and Kobiyashi equation. Further they used data from photoelasticity for finding stress field parameters by using least square method. For finding SIF they used a method of increasing the number of terms of Atluri and kobiyashi's multi parameter equation until the experimental fringes are correctly modelled. Digital image correlation (DIC) is a full field optical method used for measuring deformation, stress and strain. In DIC digital images are compared before and after deformation to get displacement field. McNeill et al. [15] determined the stress intensity factor K_I from data points (r, θ and v) obtained from 2D-DIC technique, over full field displacement field using linear least square method. They used v-displacement fields near the crack-tip and investigated the effect of using higher order terms on the evaluation of SIF. Sutton et al. [16] employed 2D-DIC to study the three-dimensional effects near the crack-tip.

In order to reduce the experimental noise, they used smoothed u-displacement and v-displacement field obtained for SEN specimen to predict the presence of three-dimensional and/or non-linear zone near the crack-tip. Han et al. [17] studied the in-plane deformation near the stationary crack-tip for thin SEN specimen using 2D-DIC. Using the multi-parameter displacement field equations derived from William's eigen function approach, they obtained the values of K_I separately, from both u-displacement and v-displacement field near the crack-tip. A total of 10 to 15 numbers of terms were used to estimate K_I from large numbers of data points. The above mentioned methodologies either neglected the error introduced due to ambiguous location of the crack-tip or used trial and error technique to locate the crack-tip that minimizes this error [16, 17]. Using the whole field displacement data (u and v) obtained from 2D-DIC, Yoneyama et al. [18] employed a non-linear least

square algorithm to estimate the mixed-mode SIF's (K_I and K_{II}), rigid body displacement as well as the location of crack-tip. They used the radial and tangential components of displacement (u_r and u_θ) derived from Atluri and Kobayashi's multi-parameter displacement field equations as a base for their mathematical formulation. They treated the displacement components separately and compared the values of K_I and K_{II} obtained from whole field displacement components u_r, u_θ, u and v. They accounted for effect of twenty terms and found that polar displacement components (u_r and u_θ) are better suited for determination of mixed mode fracture parameters as compared to Cartesian displacement components (u, v). Yoneyama et al. [1] extended the non-linear least square algorithm by using novel mathematical formulation that treats u and v displacement components in a combined way. They proposed new convergence criteria based on the correlation coefficient and the sum of absolute values of error between experimentally obtained and theoretically reconstructed displacement fields.

Yates et al. [6] found out SIF, T-stress and crack tip opening angle using DIC. They used William's approach and increased number of terms until SIF becomes constant. Gajanan et al [19] shown that DIC can be used for finding out SIF of an edge crack aligned along fiber of an orthotropic composite material. They used displacement fields, which is derived from strain fields and least square method for finding SIF. Mehdi et al. [20] experimentally found out SIF of interacting crack using photoelasticity. They used William's stress function and fitting involved Newton Raphson and least square methods.

1.2.4   Experimental and Numerical Study of Fatigue Crack Growth: XFEM and DIC

Fatigue cracking is one of the primary damage mechanisms of structural components. Fatigue cracking results from cyclic stresses that are below the ultimate tensile stress, or even the yield stress of the material. The fatigue life of a component is the the number of cycles required for the complete fracture of that component.

There are two major aspects in mixed mode fatigue crack growth: crack growth direction and crack growth rate. Various criteria for the crack growth direction under mixed mode loadings have been proposed. Some of them are maximum tangential stress criteria(MTS)

9

[21], strain energy density criteria [22, 23], dialitational strain energy density criterion [24], vector crack tip displacement (CTD) criterion [25], tangential stress factor and tangential strain factor [26] and maximum tangential strain criteria [27]. Among all these, MTS criterion is widely used. The application of this criterion can be found from the works by several authors, including Gdotos [28], Abdel [29], Chambers [27]. To correlate fatigue crack growth rates under mixed mode loading Tanaka [30] used a Paris type equation as a function of an effective stress intensity factor.

ASTM E647 [31] suggests two methods for measuring crack length. Compliance gauge method and electrical potential difference method. The compliance gauges are only useful for the straight cracks. Ali Kha Soh et al [32] used crack micro-gauge to monitor crack growth during the test. All the above methods uses electrical signals and need gauges to be attached with the specimen. Borrego et al. [33] used a traveling microscope to measure crack length. Singh et al.[34] evaluated the fatigue life of homogeneous plates containing multiple discontinuities (holes, minor cracks and inclusions) by extended finite element method (XFEM) under cyclic loading condition.

1.2.5 XFEM Modeling of Crack Propagation

Modeling of moving discontinuities such as propagating crack using conventional finite element method is highly erroneous in nature as explained earlier (see Sec. 1.2.2). XFEM enables us to model crack propagation with ease. Reinhardt et al [35] done a XFEM study on crack propagation and compared the results with experimental results.

Chapter 2

Investigation of Mixed mode Fracture Parameters for Straight, Inclined and Parallel Cracks: XFEM and DIC

2.1 Introduction

None of the literature [14, 20] has used displacement fields for finding fracture parameters for inclined and interacting cracks. In here, Atluri and Kobiyashi's multi-parameter displacement equation is used for finding SIF for many crack configurations, including inclined and interacting parallel cracks. Newton-Raphson and least square method are used for finding fracture parameters from displacement field. DIC and XFEM is used for getting displacement field, experiments and FEA respectively. Since the origin of the coordinate system for the displacement equation is at the crack tip as shown in Fig 1.2, the values of the fracture parameters depend on the coordinates of the crack tip input into the algorithm when displacement fields are used. Furthermore, the stress intensity factors cannot be estimated accurately when the coordinates of an actual crack tip are used for elasto-plastic problems. In this case, the effective crack length, where the crack tip is located at

the center of the plastic zone, should be incorporated in geometry correction. Therefore over-deterministic non-linear least square algorithm, proposed by Yoneyama et al [1] for the estimation of mixed-mode SIF's from whole field displacement field, has been implemented in a modified form. In this study, displacement data used for least square (LS) fittings is extracted along different contours from experiment/numerical analysis. To this contour data, we fit in multi-parameter displacement using least square method in a repetitive manner till we find an optimized number of terms. The procedure of optimization is carried out till the LS data fits with experimental data to a given tolerance.

2.2   Least Square Method

General procedure for the extraction of fracture parameter is represented in the form of flow chart as shown in Fig. 2.1.

For mode I, mode II and mixed mode crack in plane problems, the displacement field around a crack field is expressed as

$$
\begin{aligned}
u &= \sum_{n=1}^{\infty} \frac{A_{In}}{2G} r^{n/2} \left\{ k\cos\frac{n}{2}\theta - \frac{n}{2}\cos\left(\frac{n}{2}-2\right)\theta + \left\{\frac{n}{2}+(-1)^n\right\}\cos\frac{n}{2}\theta \right\} \\
&\quad - \sum_{n=1}^{\infty} \frac{A_{IIn}}{2G} r^{n/2} \left\{ k\sin\frac{n}{2}\theta - \frac{n}{2}\sin\left(\frac{n}{2}-2\right)\theta + \left\{\frac{n}{2}-(-1)^n\right\}\sin\frac{n}{2}\theta \right\}
\end{aligned}
\tag{2.1}
$$

$$
\begin{aligned}
v &= \sum_{n=1}^{\infty} \frac{A_{In}}{2G} r^{n/2} \left\{ k\sin\frac{n}{2}\theta + \frac{n}{2}\sin\left(\frac{n}{2}-2\right)\theta - \left\{\frac{n}{2}+(-1)^n\right\}\sin\frac{n}{2}\theta \right\} \\
&\quad - \sum_{n=1}^{\infty} \frac{A_{IIn}}{2G} r^{n/2} \left\{ -k\cos\frac{n}{2}\theta - \frac{n}{2}\cos\left(\frac{n}{2}-2\right)\theta + \left\{\frac{n}{2}-(-1)^n\right\}\cos\frac{n}{2}\theta \right\}
\end{aligned}
\tag{2.2}
$$

where, G is shear modulus, $k = (3-\nu)/(1+\nu)$ for plane stress condition and $k = (3-4\nu)$, for plane strain condition. $A_{I1}=K_I/\sqrt{2\pi}$, and $A_{II1}=K_{II}/\sqrt{2\pi}$, and $4A_{I2} = -T$ stress. In Eqs. 2.1 and 2.2, polar co-ordinates are measured from the crack tip as shown in Fig. 1.2. After accounting for rigid body motion, Eqs. 2.1 and 2.2 can be rewritten as
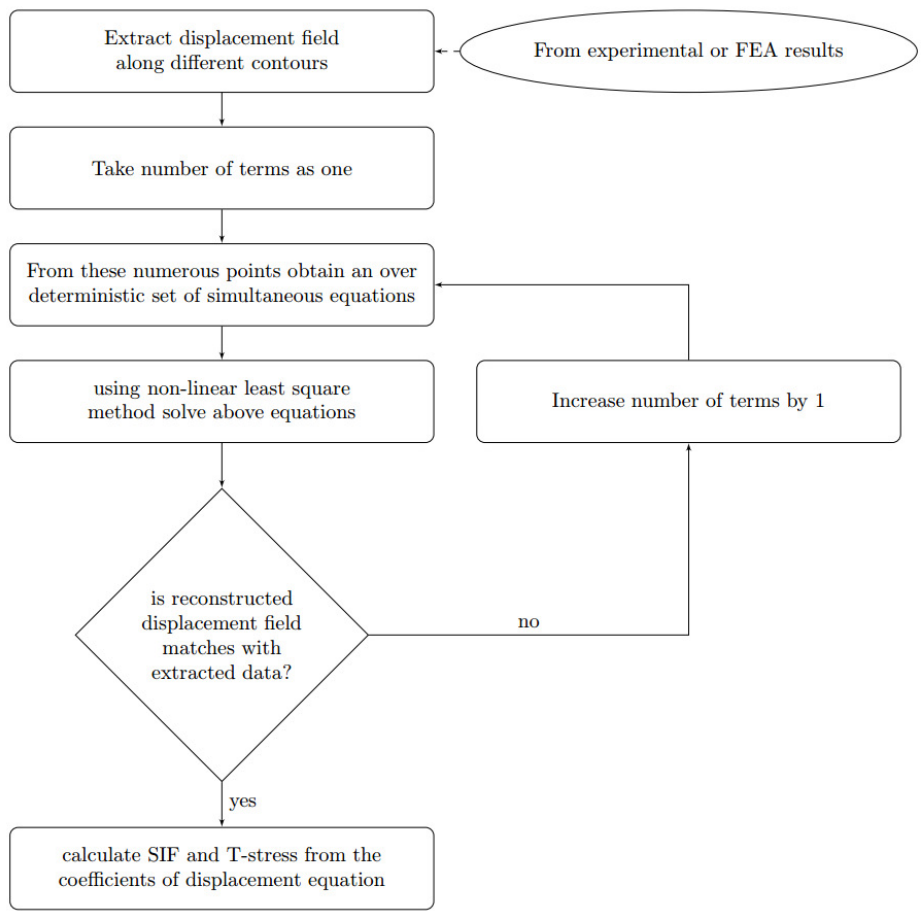
Figure 2.1: General procedure

$$u \quad = \quad \sum_{n=1}^{\infty} A_{In} f_I\left(r,\theta\right) - \sum_{n=1}^{\infty} A_{IIn} f_{II}\left(r,\theta\right) + T_x + x\left(\cos R - 1\right) - y\sin R \qquad (2.3)$$

$$v \quad = \quad \sum_{n=1}^{\infty} A_{In} g_I\left(r,\theta\right) - \sum_{n=1}^{\infty} A_{IIn} g_{II}\left(r,\theta\right) + T_y + y\left(\cos R - 1\right) + x\sin R \qquad (2.4)$$

where, f_I, f_{II}, g_I and g_{II} are trigonometric functions of position co-ordinates r and θ; T_x and T_y are rigid body translations in x and y-directions, R is the rigid body rotation. If we assume R is very small, then equations reduce to following form:

$$u = \sum_{n=1}^{\infty} A_{In} f_I\left(r,\theta\right) - \sum_{n=1}^{\infty} A_{IIn} f_{II}\left(r,\theta\right) + T_x - Ry \qquad (2.5)$$

$$v = \sum_{n=1}^{\infty} A_{In} g_I\left(r,\theta\right) - \sum_{n=1}^{\infty} A_{IIn} g_{II}\left(r,\theta\right) + T_y - Rx \qquad (2.6)$$

Although any of the Eqs. 2.3 and 2.4 or 2.5 and 2.6 can be used in the implementation, Eqs. 2.3 and 2.4 tends to increase the computational time by reducing the rate of convergence as it is non-linear in terms of unknowns T_x, T_y and R. Equations 2.5 and 2.6 is not applicable when R cannot be assumed as small angle which is especially true when the initial guesses for the required unknowns are not close to their actual values. The compromise can be achieved by incorporating simple 'if else' during the implementation of the algorithm. If $-0.15 \leq R \leq 0.15$, Eqs. 2.5 and 2.6 are used otherwise Eqs. 2.3 and 2.4 are used as a default one.

$$
\begin{aligned}
r \quad &= \quad \sqrt{(x^1 - x_c)^2 + (y^1 - y_c)^2} \\
\theta \quad &= \quad tan^{-1}\left(\frac{x^1 - x_c}{y^1 - y_c}\right) \\
x \quad &= \quad x^1 - x_c \\
y \quad &= \quad y^1 - y_c \qquad\qquad (2.7)
\end{aligned}
$$

where, x_c and y_c are the locations of a crack tip relative to an arbitrary Cartesian co-

ordinate system whose x and y-axes are parallel to that of crack tip co-ordinate system of Fig. 1.2. x^1 and y^1 are the position co-ordinates of the point of interest relative to the same arbitrary Cartesian co-ordinate system. Error function can be defined as:

$$
\begin{aligned}
h_{xm} &= u - (u)_{exp} \\
h_{ym} &= v - (v)_{exp}
\end{aligned}
\tag{2.8}
$$

Applying Taylor series expansion

$$
\begin{aligned}
(h_m)_{i+1} &= (h_m)_i + \frac{\partial h}{\partial A_{I1}}(\nabla A_{I1}) + ... + \frac{\partial h}{\partial A_{II1}}(\nabla A_{II1}) + ...\frac{\partial h}{\partial T_x}(\nabla T_x) + \frac{\partial h}{\partial T_y}(\nabla T_y) \\
&+ \frac{\partial h}{\partial R}(\nabla R) + \frac{\partial h}{\partial x_o}(\nabla x_o) + \frac{\partial h}{\partial y_o}(\nabla y_o)
\end{aligned}
\tag{2.9}
$$

where $i = i^{th}$ iteration step and ∇A is the correction to be added to the previous estimate of A

To determine corrections take $(h_m)_{i+1} = 0$

$$
\begin{aligned}
-(h_m)_i &= \frac{\partial h}{\partial A_{I1}}(\nabla A_{I1}) + ... + \frac{\partial h}{\partial A_{II1}}(\nabla A_{II1}) + ...\frac{\partial h}{\partial T_x}(\nabla T_x) + \frac{\partial h}{\partial T_y}(\nabla T_y) \\
&+ \frac{\partial h}{\partial R}(\nabla R) + \frac{\partial h}{\partial x_o}(\nabla x_o) + \frac{\partial h}{\partial y_o}(\nabla y_o)
\end{aligned}
\tag{2.10}
$$

Rearranging in matrix form

$$
\begin{aligned}
\{h_i\} &= -[b]_i \{\nabla A\}_i \\
\{\nabla A\}_i &= -[c]_i^{-1} \{d\}_i
\end{aligned}
\tag{2.11}
$$

where, $[c]_i = [b]_i^T [b]_i$, and $\{d\}_i = [b]_i^T \{h\}_i$

The Eq. 2.11 gives the correction terms for prior estimates of the coefficients. Accordingly an iterative procedure must be used to get best fit sets of coefficients. Then the estimates of the unknowns are revised as

15

$$\{A\}_{i+1} = \{A\}_i + \{\nabla A\}_i \tag{2.12}$$

The above equations are solved using Newton-Raphson scheme in an iterative manner. The iterations are stopped using two criteria, namely: (a) Parameter error (ΔA) minimization (b) minimization of displacement vector sum error which is defined as

$$\frac{\sum | u_{theory} - u_{exp} |}{\text{Total number of data points}} \leq \text{convergence error} \tag{2.13}$$

where, u_{theory} is vector sum of theoretically recalculated u and v-displacements and u_{exp} is vector sum of experimental u and v-displacements.The solution for the given number of parameters is considered as acceptable when the convergence error is of the order of 0.001 and parameter error ∇A becomes reasonably small. Number of terms required in multi-parameter displacement field equations to model the displacement field correctly, is incremented from 1 until the reconstructed u and v displacement field matches with experimental distribution. The cross checking is done by plotting theoretically reconstructed u and v displacement contour maps over the displacement data which is used for least square fitting. The algorithm is validated by applying it to both experimental and numerical displacement field. For getting displacement fields, experiment is done using digital image correlation.

2.3   Fracture parameters from experimental displacement field

Experimental techniques that measure the surface deformation of components and structures, subjected to a variety of loading conditions, play an important role in many areas of engineering. DIC is established in the field of experimental mechanics as an effective and flexible tool for the full field measurement of shape and deformation. This is due to the range of advantages DIC offers over the other experimental techniques such as simple optical set up, ease of specimen preparation, relatively less stringent requirements on measurement conditions and wide range of sensitivity of measurement. We used a single recording camera (2D-DIC), it can measure in-plane surface displacement of a planar object. Experiments
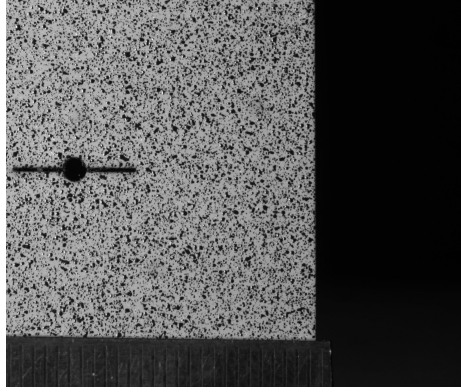
Figure 2.2: Specimen with speckle pattern for digital image correlation

are conducted on the test specimens machined from 3 mm thick sheet of aluminum alloy (Al2014-T6). Wire cut EDM is used for machining and creating crack. In order to simulate the natural crack, test specimens are pre-cracked in fatigue loading condition using MTS Landmark® servo-hydraulic cyclic testing machine of 100 kN capacity. Care is taken while locating and securing the specimens in the hydraulic test fixtures so as to have approximately similar fatigue crack growth behavior on both the sides of the specimen. During the pre-cracking process, the specimen is monitored closely with magnifying glass. Liquid dye-penetrant NDT-19 is used to detect any fatigue crack initiation. Fatigue pre-cracking is conducted using force control mode and a short crack of the approximate length of 0.5-1 mm is obtained for the test specimens. Using optical microscope, lengths of the cracks are measured on both the sides of the specimens and total crack-length is obtained by averaging the values of measured crack lengths on both the sides of the specimen. Then, the pre-cracked test specimens are cleaned thoroughly with isopropyl alcohol. The surface of the specimens are coated with a thin layer of white acrylic paint and over-sprayed with carbon black paint using an airbrush to obtain a random black-and-white speckle pattern.

Table 2.1: Material properties of Al2014T6 alloy

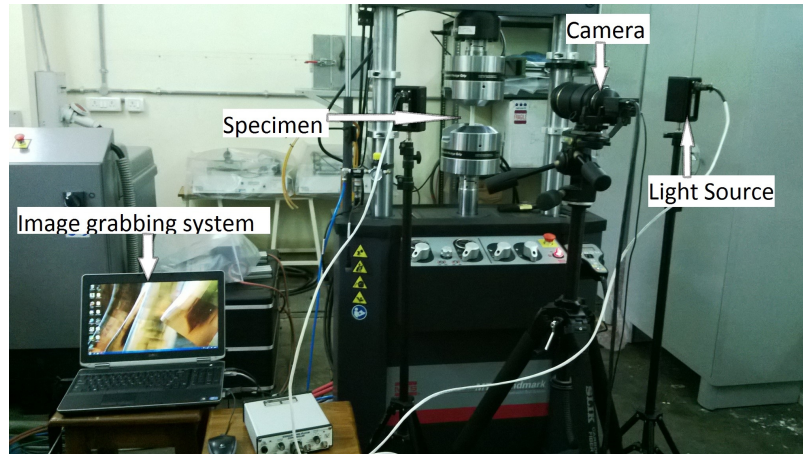| Property	Value
Young's modulus, GPa	72400
Poisson's ratio ν	0.33

17

Figure 2.3: Experimental setup for 2D DIC experiment

Figure 2.3 shows the typical 2D DIC experimental setup. The hardware for the optical setup of 2D-DIC system comprises a CCD camera (of 2448 2048 spatial resolution with 8 bit intensity resolution and frame rate of 15 fps), Tamron lens with 180mm focal length, a portable computer system with image acquisition card and LED lighting to ensure adequate image contrast. All the experiments are performed using a computer-controlled MTS Landmark$^®$ servo-hydraulic cyclic testing machine of 100 KN capacity with a computer data acquisition system. Self-adjusting hydraulic test fixtures are used to grip the specimens.

The experimental procedure starts with the specimen fixing into hydraulic wedge grips and specimen straightness is ensured using a try square. A camera is mounted on a tripod and the horizontal level of the camera is checked using spirit level and adjusted accordingly. Height of the camera is adjusted in the tripod to ensure full view of the specimen. The camera is aligned with respect to the specimen and positioned. The distance between the camera and the specimen is adjusted depending on the specimen area to be captured. Positions of LED lamps are adjusted to get uniform illumination of the specimen surface. The surface of interest is focused by adjusting the lens to get a sharper speckle pattern. The aperture of the lens is adjusted to get sufficient intensity and also to avoid saturation of the pixels over the field of view. Finally images are grabbed at a rate of ten images per second while the uniaxial tensile load is applied along longitudinal direction of the test specimens

using displacement control mode with a cross-head speed of 0.5 mm/min .While grabbing the images the output from the load cell is synchronized with images for obtaining the load value using data acquisition systems. Post-processing of the acquired images is done by using VIC-2D 2010 software acquired from Correlated Solutions. The region of interest (ROI) is selected and the subset sizes are chosen as 35x35 and a step size of 5 is taken. The data got after post processing is smoothed to get smooth continuous contours with a filter size of 37. For calculating SIF data extracted from contours by drawing lines over the contour and VIC-2D is used to extract data from the line. Data is collected from the annular region surrounding the crack-tip, the inner radius of which is chosen more than 1.5 times of the specimen thickness to avoid the three-dimensional effects and non-linear process zone in the vicinity of the crack tip [5]. The outer radius of the annular data collection region is limited such that $r/a \leq 1$. Total 1000-1300 data points are collected from a specimen. An over-deterministic non-linear least squares procedure is then invoked using MATLAB program to evaluate the multiple parameters governing the displacement field. Experiment is done on single edge notch specimens and results are compared with analytical results.

2.3.1 Single edge notch(SEN)

To understand the algorithm correctly, we explain the procedure in detail with this example. For the later examples we only give the results and corresponding graphs. The process starts with collecting data for least square method from three or more contours as shown in Fig. 2.5(a). The data should be taken from both u and v displacement fields. The data which are collected (Fig. 2.5(b)) is used for least square fittings for finding parameters and then with that parameters u and v contours are plotted with data points echoed back. We start the algorithm with a number of terms, one for each first and second term of multi-parameter equations and checked the similarity of collected data and reconstructed data. If they are not matching we increase the number of terms of multi-parameter equations by one until the contours matches reasonably. Figure 2.6 shows the theoretically reconstructed displacement field around the crack tip of SEN specimen (subjected to a load of 10 kN) obtained using various parameters with the data points echoed back (indicated by red colored marker dots). The data points coincide very well with reconstructed contours as the number of parameters
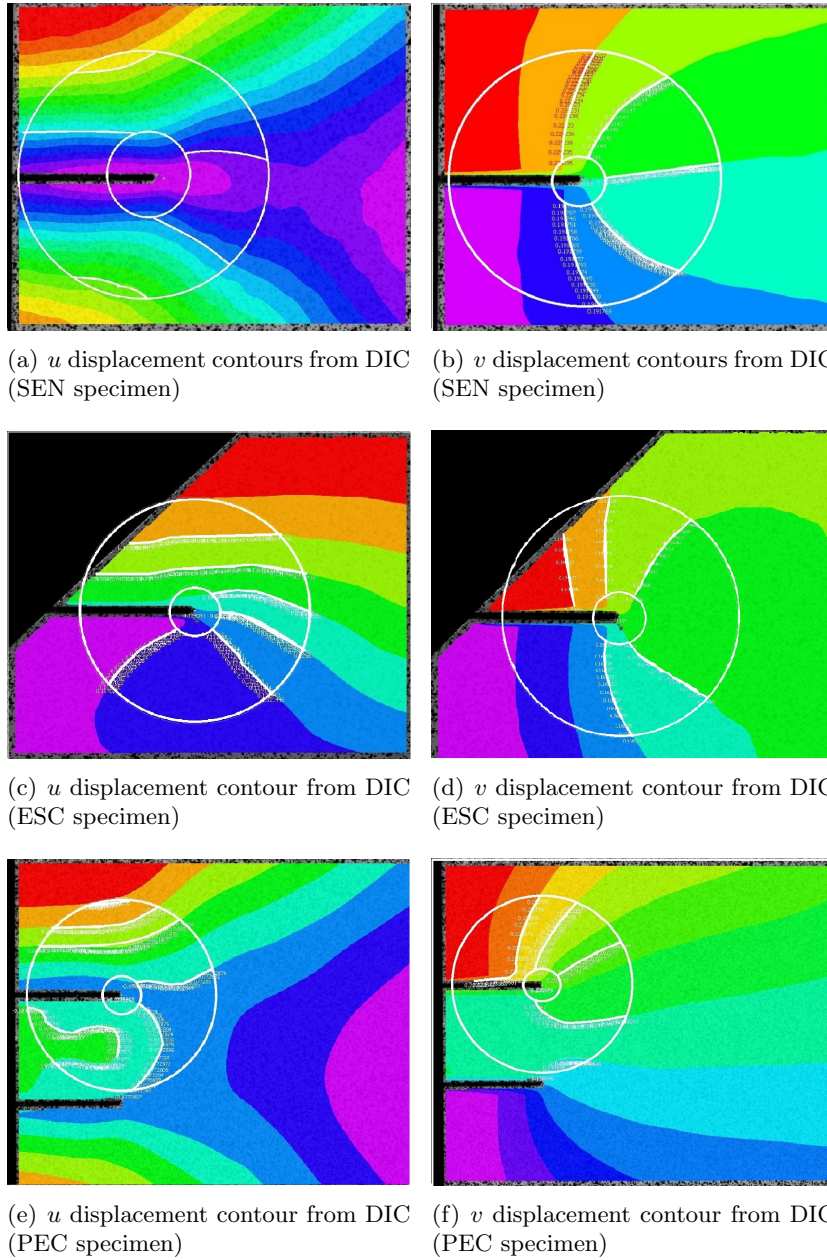
(a) u displacement contours from DIC (SEN specimen)

(b) v displacement contours from DIC (SEN specimen)

(c) u displacement contour from DIC (ESC specimen)

(d) v displacement contour from DIC (ESC specimen)

(e) u displacement contour from DIC (PEC specimen)

(f) v displacement contour from DIC (PEC specimen)

Figure 2.4: DIC images with contours used for LS fitting (shown white in color inside circle)
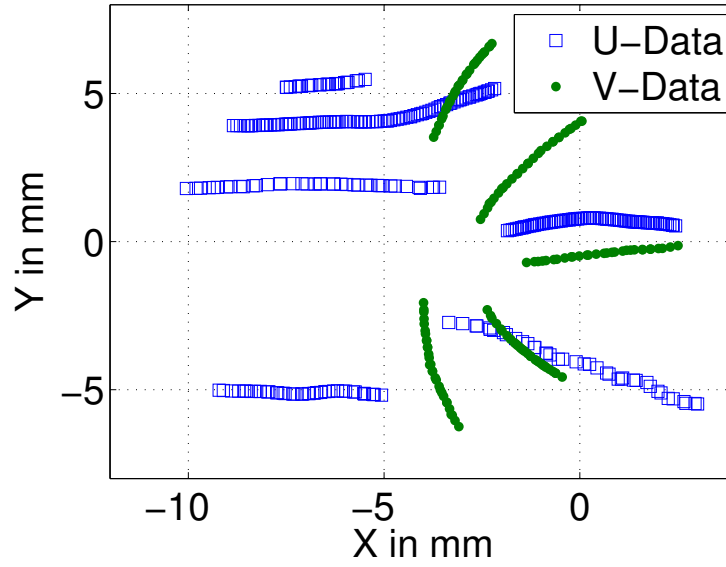
Figure 2.5: Data points from which u and v displacements are taken for least square fitting (SEN specimen)

increases to six, assuring the sufficiency of six parameters to represent the displacement field. Comparing K_I with its analytical value, the error is around 2.3%. The sample dimension of SEN is given in the Fig. 2.9.

Table 2.2: Fatigue pre-cracking

Type	Initial notch length (mm)	Final crack length (mm)	Mean load KN	Amplitude of load KN	Number of cycles	Frequency Hz
SEN	8	8.5	4	3	7805	5
ESC	8	8.556	3.5	3	20000	10
PEC	8	8.58	3	3	18000	10

Table 2.3: SEN at 10 kN load

	2 para	3 para	4 para	5para	6 para	Analytical	%error
K_I, $MPa\sqrt{mm}$	562	567.5	592	586.32	588.61	602.8	2.3
K_{II}, $MPa\sqrt{mm}$	14	17	1.5	14	16	0	

2.3.2 Edge Slant Crack(ESC)

The coordinate system for the multi-parameter equation is in such a way, that the x-axis should be parallel to the crack. In experiments to align crack along x-axis, the camera
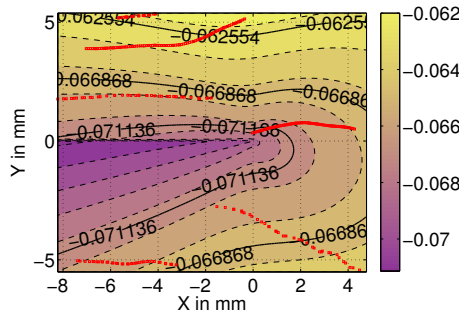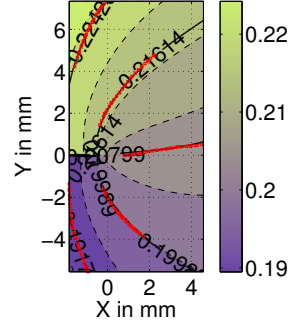
(a) u displacement contour for the 1 parameter solution with data points echoed back(red in colour)
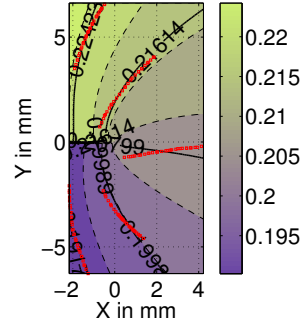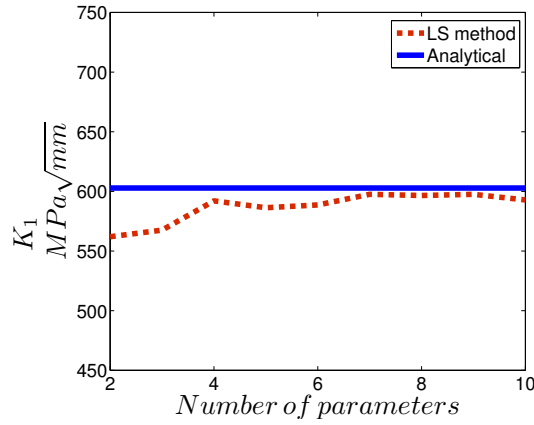
(b) v displacement contour for the 1 parameter solution with data points echoed back(red in colour)
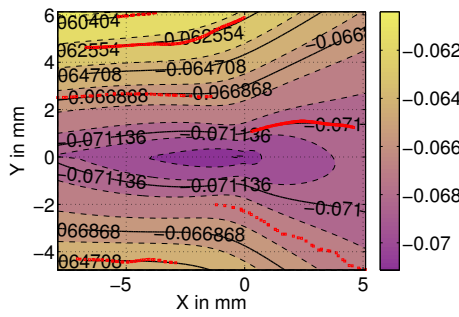
(c) u displacement contour for the 6 parameter solution with data points echoed back(red in colour)

(d) v displacement contour for the 6 parameter solution with data points echoed back(red in colour)

(e) Variation of K_I with number of parameters

Figure 2.6: Results obtained from the experimental displacement field of a SEN specimen

should be tilted such that x-axis is parallel to the crack. The images taken for the inclined crack is shown in figure. Analysis is done on edge slant cracked specimen at 10 kN force. Results are compared with analytical results

Table 2.4: ESC at 10 kN load

	LS Fitting	Analytical	%error
$K_I, MPa\sqrt{mm}$	303	302.43	.18
$K_{II}, MPa\sqrt{mm}$	187.5	183.6	2.18

2.3.3 Parallel crack

Analysis is done on a parallel cracked specimen at 10KN force. Results are compared with numerical results. XFEM is used for modelling the crack. Since the specimen is symmetric, we need to model only the half part of the specimen. The XFEM model is shown in figure

Table 2.5: PEC at 10 kN load

	LS Fitting	ABAQUS	%error
$K_I, MPa\sqrt{mm}$	442.9	506.3	12.45
$K_{II}, MPa\sqrt{mm}$	-69.6	-66.1	5.7

## 2.4 Fracture parameters from Numerical Displacement Field

The extended finite element method (XFEM) is used for modelling crack in numerical method. XFEM alleviates shortcomings associated with the meshing of crack surfaces in existing methods. In this method, the finite element approximation is enriched by additional functions through the notion of partition of unity. The essence of the XFEM lies in sub-dividing a model problem into two distinct parts: mesh generation for the geometric domain (cracks and holes not included), and enriching the finite element approximation by additional functions that model the flaws and other geometric entities. In this work we used XFEM capability of ABAQUS to model the cracked panels. Since XFEM is not much dependent on meshing, fine incremental type of meshing which we usually use for conventional finite element method is not required for modeling cracks. In ABAQUS we
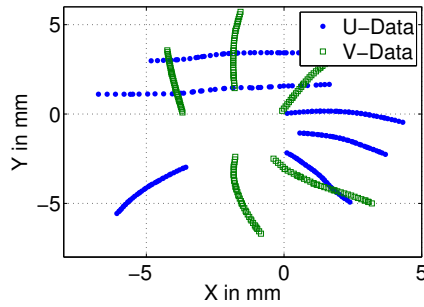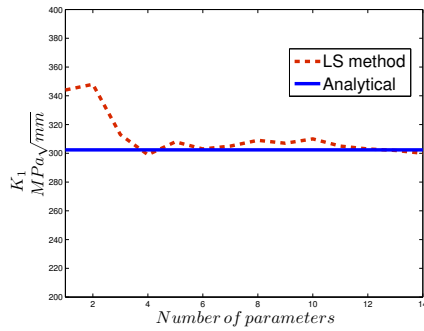
(a) Data points from which u and v displacements are taken
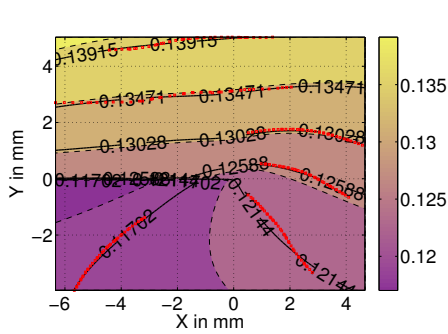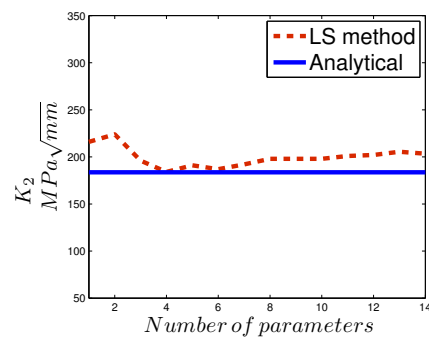

(b) u displacement contour for the 6 parameter solution with data points echoed back(red in colour)
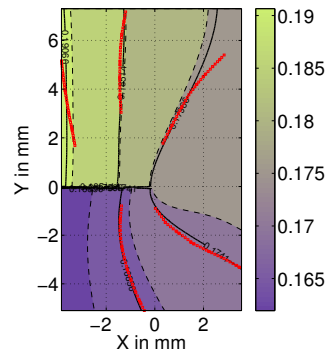
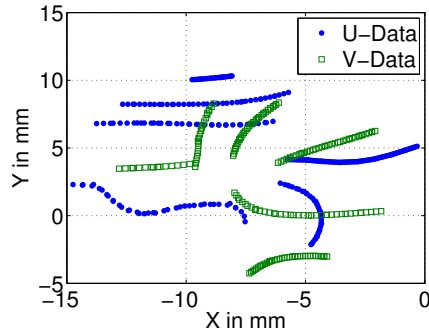(c) v displacement contour for the 6 parameter solution with data points echoed back(red in colour)

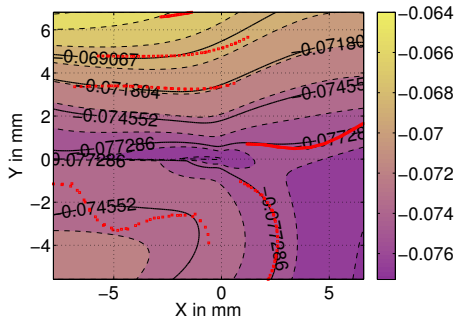(d) Variation of K_I with number of parameters

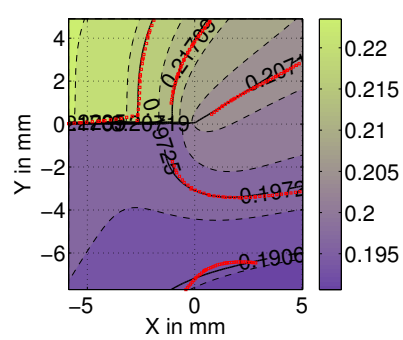(e) Variation of K_{II} with number of parameters

Figure 2.7: Results obtained from a experimental displacement field of a edge slant crack (ESC) specimen
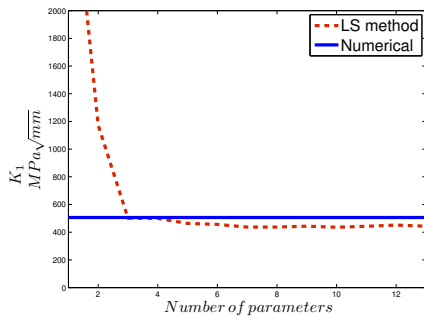
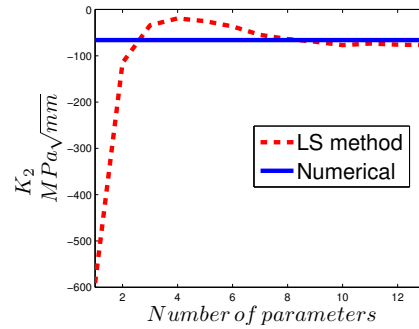(a) Data points from which u and v displacements are taken

(b) u displacement contour for the 9 parameter solution with data points echoed back(red in colour)

(c) v displacement contour for the 9 parameter solution with data points echoed back(red in colour)

(d) Variation of K_I with number of parameters

(e) Variation of K_{II} with number of parameters

Figure 2.8: Results obtained from a experimental displacement field of a parallel crack (PEC) specimen

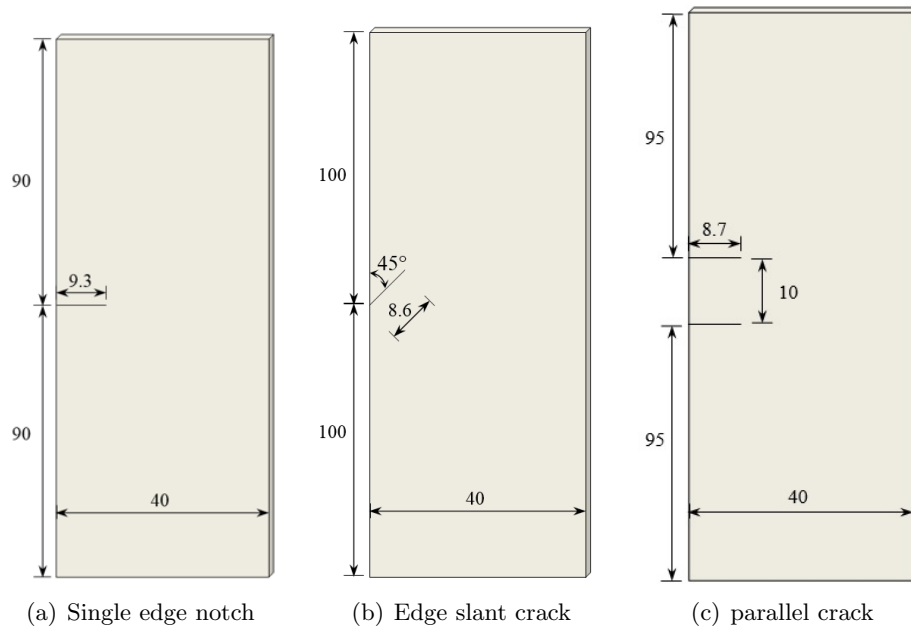|		
(a) Single edge notch	(b) Edge slant crack	(c) parallel crack

Figure 2.9: Dimension of different models which are used for XFEM modelling

can mesh the plate without crack and then it is possible to assemble the geometry of the crack which we needed to the plate. Considering computational easiness and number of data points required for the least square fitting the panel is partitioned and gave a fine mesh near to the crack tip and a coarse mesh away from the crack tip. Hexagonal elements are used for the meshing. Properties of Al 2014-T6 alloys are used for modeling. Fix top end and $u = 0$ for the bottom end are taken as the boundary conditions. Force in the form of pressure is applied on the bottom surface. The nodal coordinates and the corresponding u and v displacement values are extracted from the ABAQUS. A MATLAB program is used to collect data along contours which is used for the least square fitting. The algorithm is verified with many configurations such as Single edge notch (SEN), edge slant crack (ESC), parallel interacting crack (PEC).

2.4.1   Single edge notch

To validate the algorithm for pure mode-I problems, the analysis is done on a SEN specimen. Dimensions of the SEN model are given Fig. 2.9. With 8 term equation the reconstructed and numerical data matches closely as shown in Fig. 2.10.
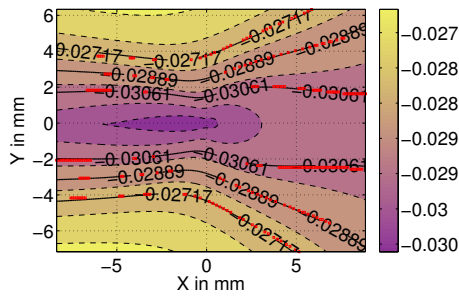
Table 2.6: SEN at 7.5KN load

	LS Fitting	ABAQUS	%error
K_I, $MPa\sqrt{mm}$	487	492	1.016
K_{II}, $MPa\sqrt{mm}$	6	0	-
σ_{0x}, MPa	-32	-26	23
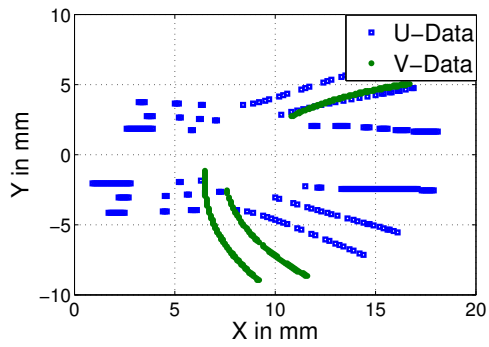
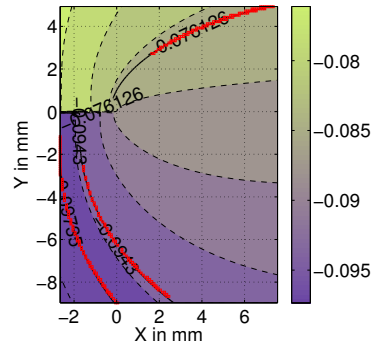(a) Data points from which u and v displacements are taken
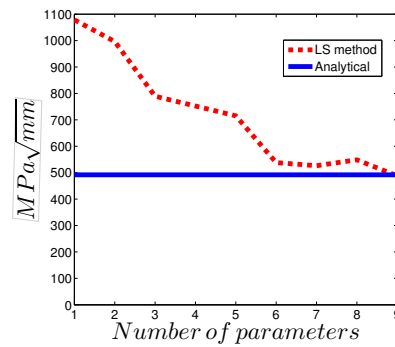
(b) Variation of K_I with number of parameters

(c) u displacement contour for the 8 parameter solution with data points echoed back(red in colour)

(d) v displacement contour for the 8 parameter solution with data points echoed back(red in colour)

Figure 2.10: Results obtained from the XFEM displacement field of a SEN specimen

27

Table 2.7: ESC at 10kN load

|	LS Fitting	ABAQUS	%error
K_I, $MPa\sqrt{mm}$	326	344	5.5
K_{II}, $MPa\sqrt{mm}$	169	188	10
σ_{0x}, MPa	-32	-37	13.5

2.4.2 Edge slant crack

To validate our algorithm for the mixed mode problems, analysis is done on an ESC speci-
men. Since the coordinates of the multi-parameter equation is as shown in Fig. 1.2, we need
to apply a coordinate transformation. Dimensions of the ESC model are given Fig. 2.9. With
8 number of terms the reconstructed contours closely matches with numerical data(Fig. 2.7).
So the parameters corresponding to 8 number of terms is taken as results. Table 2.7 shows
K_I , K_{II} and T-stress and these are matching reasonably with the numerical results ob-
tained directly from XFEM.

2.4.3 Parallel crack

The validity of algorithm for interacting crack is checked on a model with dimensions as
shown in Fig. 2.9. With 10 terms in equation the reconstructed displacement field matches
with extracted displacement data. The SIFs values obtained by least square fitting and
XFEM matches very closely as shown in the Table 2.8. The variation of SIF with number
of terms used and displacement plot is shown in Fig. 2.12.

Table 2.8: PEC at 7.5KN load

	LS Fitting	ABAQUS	%error
K_I, $MPa\sqrt{mm}$	367.4	370	.7
K_{II}, $MPa\sqrt{mm}$	46	52	11
σ_{0x}, MPa	-56	-54	3.7
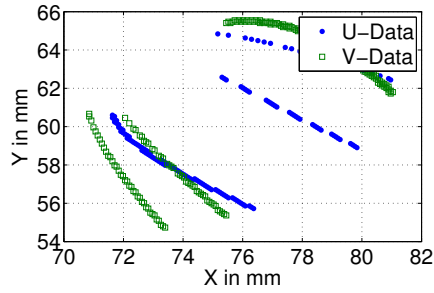
(a) Data points from which u and v displacements are taken
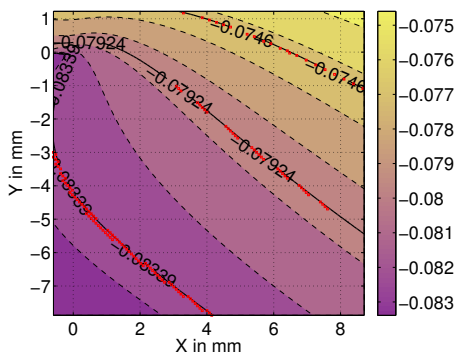
(b) u displacement contour for the 6 parameter solution with data points echoed back(red in colour)
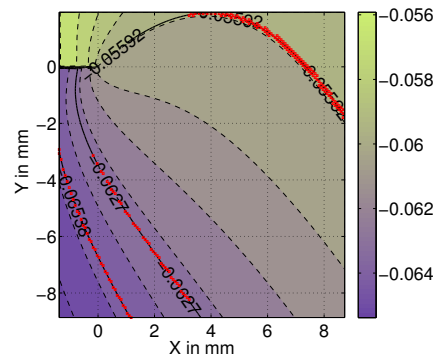
(c) v displacement contour for the 6 parameter solution with data points echoed back(red in colour)

(d) Variation of K_I with number of parameters

(e) Variation of K_{II} with number of parameters

Figure 2.11: Results obtained from a XFEM displacement field of a edge slant crack(ESC) specimen
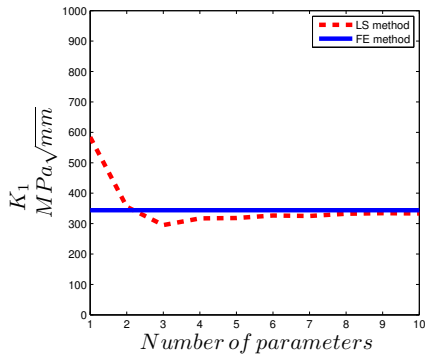
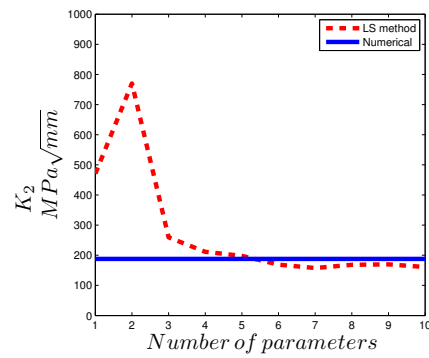(a) Data points from which u and v displacements are taken

(b) u displacement contour for the 10 parameter solution with data points echoed back(red in colour)

(c) v displacement contour for the 10 parameter solution with data points echoed back(red in colour)
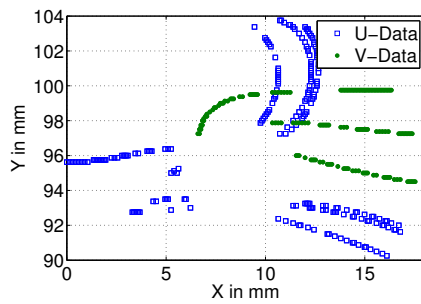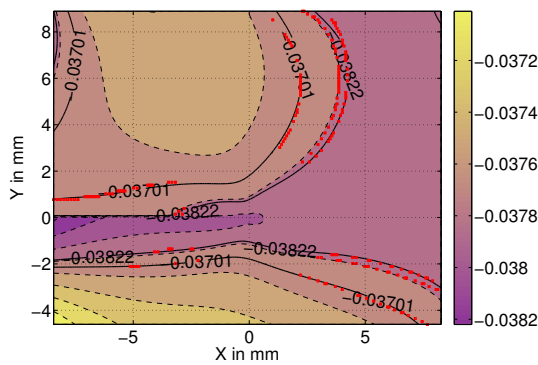

(d) Variation of K_I with number of parameters

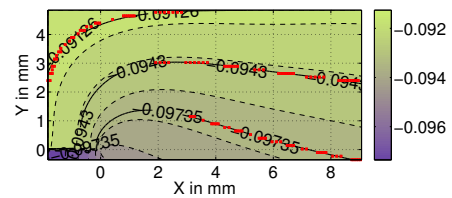(e) Variation of K_{II} with number of parameters

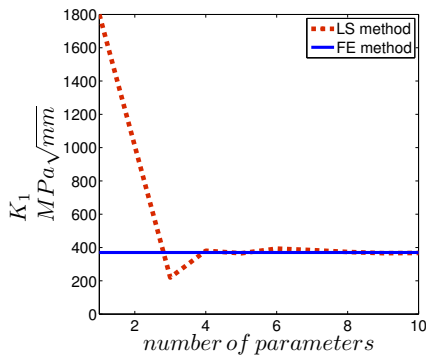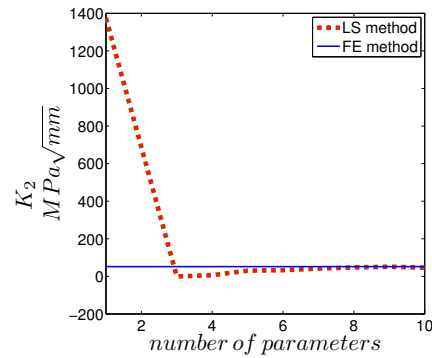Figure 2.12: Results obtained from the numerical displacement field of a parallel cracked (PEC) specimen

2.5 Conclusion

The proposed method is used for analyzing the following crack configurations.

a) straight crack

b) Inclined crack

c) Parallel crack

for fracture parameters from both experimental and numerical displacement field.

Using least square algorithm we fitted displacement fields (with respect to local coordinates) and found that 6 parameter solution is optimum for representing inclined crack and straight crack displacement fields. From fitted displacement fields we have extracted SIF and T-stress. Using this we validated that the optimized displacement field can be used for mixed mode problems for finding fracture parameters. Then we extended this method for parallel crack in which two parallel edge cracks are separated by distance d. In parallel cracks the crack experience mode mixicity due to interactions. Using the same least square algorithm we obtained the displacement field shows that upto 12 number of terms are needed to represent displacement field for parallel crack. In the case of interacting cracks, we observed that more number of parameters in multi-parameter equations is needed to get a fitted displacement field.

K_I and K_{II} evaluated from the displacement field obtained from the experiments, of SEN and ESC crack shows a maximum percentage error of 2.3%. But in the case of parallel crack K_I and K_{II} shows 12.14% and 5.7% respectively which is higher than the error observed in SEN and ESC. K_I and K_{II} evaluated from the displacement field obtained from the XFEM analysis, of an elastic model, of SEN and ESC crack shows a maximum percentage error of 10%. The elastic modeling can't represent crack problem realistically. If we use elastic-plastic model, the crack will be more realistic and the error in parameters may come down. In the case of parallel crack K_I and K_{II} show .7% and 11% respectively. T-stress shows 23%, 13.5% and 3.7% error for SEN, ESC and PEC respectively. This errors obtained for T-stress is higher than that of stress intensity factors. From this work, it is evident that the displacement field is useful for finding stress intensity factors.

Chapter 3

Prediction of Fatigue Life of Edge Cracked Aluminium Plate: XFEM and DIC

3.1 Introduction

Fatigue cracking is one of the primary damage mechanisms of structural components. Fatigue occurs when a material is subjected to repeated loading and unloading. If the loads are above a certain threshold, microscopic cracks will begin to form at the stress concentration points. Eventually a crack will reach a critical size, the crack will propagate suddenly, and the structure will fracture. The fatigue life of a component can be expressed as the number of loading cycles required to initiate a fatigue crack and to propagate the crack to critical size. Therefore, it can be said that fatigue failure occurs in three stages crack initiation; slow, stable crack growth; and rapid fracture.For some components the crack propagation life is neglected in design because stress levels are high, and/or the small critical flaw size. For other components the crack growth life might be a substantial portion of the total life of the assembly.

None of the literatures used digital image correlation for measuring crack growth. Digital image correlation (DIC) is a full field optical method used for measuring deformation, stress

and strain. In DIC digital images are compared before and after the deformation to get displacement field. In this work we are proposing a method for monitoring crack growth using digital images. Numerical simulation is done using ABAQUS 6.9 which has inbuilt XFEM module in it. We also studied the effect of mode mixity in the life of edge cracked aluminum specimens.

3.2   Experimental Study

In this work DIC is used for monitoring crack growth. The method for specimen preparation is the same as explained in Sec. 2.3. Since we can identify when the crack starts from the images, pre-cracking is not necessary for generating natural crack. In experimental setup, apart from the image grabbing system everything is same as explained in the Sec. 2.3.

The image grabbing system for the fatigue experiments comes with a triggering controller. In order to get exact correlations between the images and number of cycle, camera triggering controller is used which will trigger the camera in equal intervals of cycles and also at specified phase angles. In the present analysis the images were captured every twenty cycle and at every 90 degree phase angle.While grabbing the images the output from the load cell is synchronized with images for obtaining the number of cycles using data acquisition systems. The reference image is calibrated for a known distance such that it will enable one to get coordinates of any pixel in mm. This capability of image correlation is used for obtaining the crack advancement distance from the crack tip. Post-processing of the captured images is done using VIC-2D 2010 software acquired from Correlated Solutions. The region of interest (ROI) is selected and the subset sizes are chosen as 35x35 and a step size of 5 is taken. The x and y coordinate plots are used for measuring crack length and propagation angle. The crack length and the propagation direction is calculated using Eqs. 3.1 and 3.2 respectively.

$$\triangle a = \sqrt{(x_{ci} - x_c)^2 + (y_{ci} - y_c)^2} \tag{3.1}$$

33

$$\theta = \arctan \frac{y_c - y_{ci}}{x_c - x_{ci}} \tag{3.2}$$

where

θ is crack propagation direction

x_{ci} and y_{ci} are the coordinates of the initial crack tip

x_c and y_c are the current tip coordinates

3.3 Numerical method XFEM

In the present work, the fatigue crack growth simulations are performed by XFEM. Mixed mode stress intensity factor is extracted from J-integrals. The direction of crack propagation is established to be a function of the mixed-mode stress intensity factor of the crack tip. There are several criteria to calculate the direction. Some of the most widely used mixed mode criteria are; the maximum tangential stress criterion, the maximum energy release rate criterion, the zero k_2 criterion and maximum circumferential stress criterion. In this study we have been using maximum tangential stress criterion [21] in which the deflection angle of crack growth defined to be perpendicular to the maximum tangential stress at the crack tip. The crack propagation angle θ is given by the Eq. 3.3. where the crack propagation angle θ is measured with respect to the crack plane $\theta = 0$ and represents the crack propagation in the straight-ahead direction. $\theta < 0$ if $k_2 > 0$ while $\theta > 0$ if $K_2 < 0$

$$\theta = \arccos(\frac{3K_{II}^2 + \sqrt{k_I^4 + 8k_1^2 + k_{II}^2}}{K_I^2 + 9K_{II}^2}) \tag{3.3}$$

For mixed mode crack growth problems we use equivalent mode 1 SIF for the life calculations. Tanank [30] proposed a formula for the equivalent SIF based on curve fitting data.

$$\triangle K_{eq} = \sqrt[4]{\triangle K_I^4 + 8\triangle K_{II}^4} \tag{3.4}$$

34

where

$$\triangle K_1 = K_{Imax} - K_{Imin} \tag{3.5}$$

$$\triangle K_2 = K_{IImax} - K_{IImin} \tag{3.6}$$

For stable crack propagation, the generalized Paris law is described as

$$\frac{da}{dn} = C \left(\triangle K_{equ}\right)^m \tag{3.7}$$

where, a is the crack length, N is the number of loading cycles and K_{eq} is obtained by with $\triangle K_I$ and $\triangle K_{II}$, C and m are material properties. The loading cycles required to extend the crack from initial length to final failure length are evaluated by Eq. 3.7. A compromise must be made regarding the value of the linear extension length $\triangle$a. If crack increments are too small, then very fine meshing is required at the crack tip so that the new crack tip should fall in new elements after each step. If increments are too long, the piece wise linear paths cannot precisely represent the real crack path. The problems having single crack, $\triangle a$ is kept constant.

3.4 Experimental and numerical validation

3.4.1 problem Definition

In this work we are investigating the crack growth behavior of thin edge cracked aluminum 2014-T6 alloy panels. The material properties and Paris law constants of the AL2014T6 [36] are given in the Table 3.1 and 3.2 respectively.

Table 3.1: Material Properties of AL2014-T6

Property	Value
Young's modulus, GPa	73.1
Poisson's Ratio	0.33

We have taken two configurations of crack which represent mode 1 and mixed mode crack growth behavior.

Table 3.2: Paris Law Constants of AL2014-T6

Property	Value
C, mm/(cycle*MPa$\sqrt{mm}$)	5.57e-13
m	3.37

1) Side Edge notched specimen (SEN)

2) Edge slant cracked specimen (ESC)

The experiment is conducted on a 3 mm thick sheets of aluminum alloy. The dimensions of the specimen is given in the Fig. 3.1. A fatigue load in sinusoidal forms is applied to the both specimens. The specifications of the load is given in the Table 3.3. The crack behavior is investigated using DIC and XFEM.

Table 3.3: Fatigue load

Property	Value/Type
Mean load, kN	5
Amplitude, kN	3.5
Frequency, Hz	10
Applied form	Sinusoidal

3.4.2 Experimental evaluation

In usual procedure in order to simulate natural crack, pre-cracking is done. While we use DIC for measuring crack growth we can monitor the images, and when the crack starts to grow that is image is taken as first image. The images are correlated. the crack growth and number of cycles are extracted such that $\triangle a$ should be less than 2mm. In the cases of SEN and ESC crack the crack grows almost in x direction. So we have taken $y_{ci} = y_c$. Then $\triangle a$ becomes $x_{ci} - x_c$ and $\theta = 0$ in global coordinates.

3.4.3 Numerical Technique (XFEM)

In the present work, ABAQUS 6.9 which has inbuilt XFEM module in it is used for numerical simulations. We used a 3-D model to extract SIFs. XFEM module for modeling crack enables us to create the crack geometry separately and assemble the crack to the plate. We meshed the plate with two elements along the the thickness. SIF and crack propagation
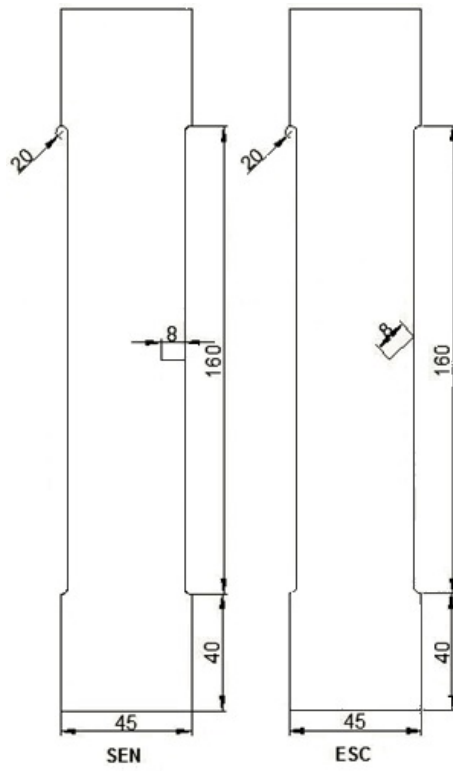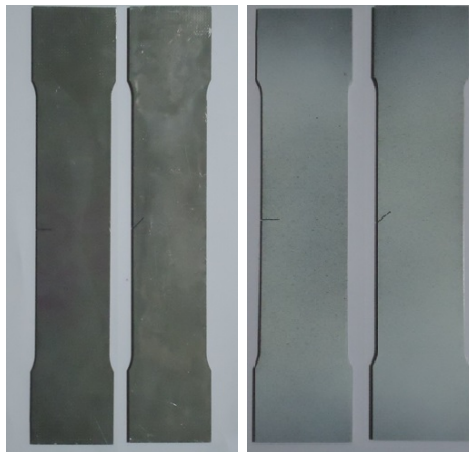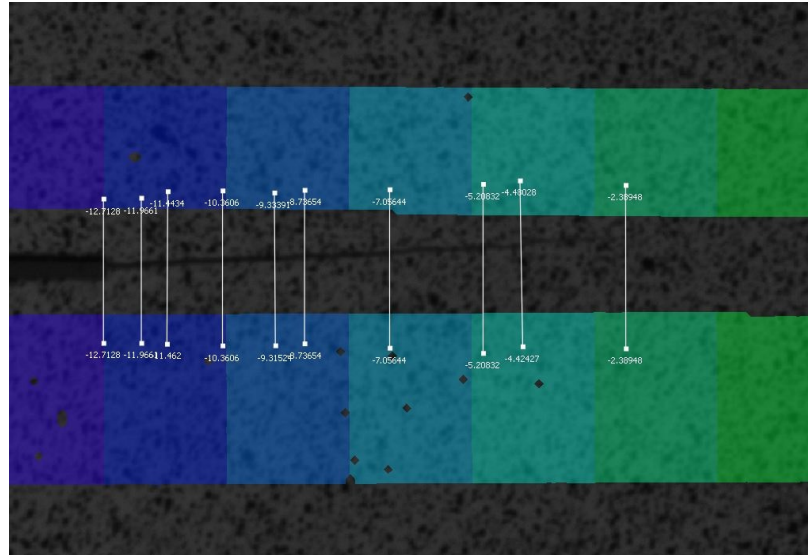
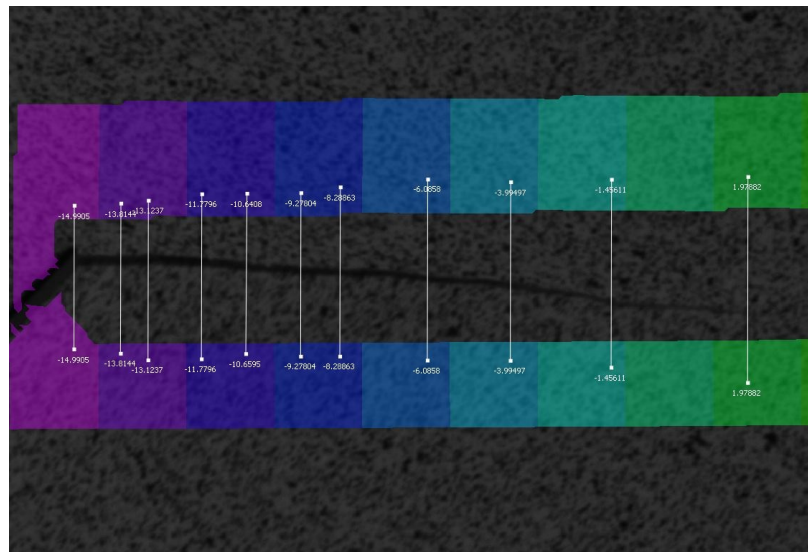Figure 3.1: Specimen Dimensions

(a) Without speckle   (b) with speckle

Figure 3.2: Work pieces

(a) DIC images of SEN

(b) DIC image of ESC specimen

Figure 3.3: DIC images with lines at various crack tip points

direction is evaluated from the mid-plane of the model. For simplify the crack modeling, the crack propagation direction is approximated to the nearest integer. The life for the crack increment is calculated using Paris law The crack length is incremented by 0.5 mm in the crack propagation direction and the new SIF and crack propagation direction are extracted. This process continued until the plate fails.

## 3.5   Results and Discussions

Experimental and numerical study of specimens are done. Life estimated using XFEM matches very closely with experimentally observed life as given in Table 3.4. Fatigue life diagrams are shown in 3.4(a) and 3.4(b). The XFEM and the experimental life diagram are matches very closely. Even though we used same loads and crack length the life of ESC specimen is more than double of the SEN specimen. The life of SEN and ESC specimen is shown as bar graph in Fig. 3.4(c).

Since it is little difficult to identify the crack tip precisely from the images, advised to put some paint in the crack, such that it can flow through the crack as it grows. Then crack tip identification will be pretty easier. While using XFEM for numerical modeling, very fine mesh is advised near the mixed mode crack tip so that we should get enough number of contours within the crack increment.

In this work, digital images are used for measuring crack length. When we use a moving microscope, it is necessary to stop the experiment to measure the crack length. In that case, strict monitoring of crack is required to stop loading cycle and to take measurements. But if we use an image grabbing system with a triggering controller the images are taken in the regular interval of cycles. So the crack length can be measured very easily from that images, without interrupting loading cycle. Further more, the experimental set up does not contains any component which is directly attached to the specimen. So the setting up of experiment is relatively easy compared with other experiments such as compliance gauge method and electrical potential difference method. Due to above mentioned advantageous, the crack monitoring using DIC is found to be easy and useful.
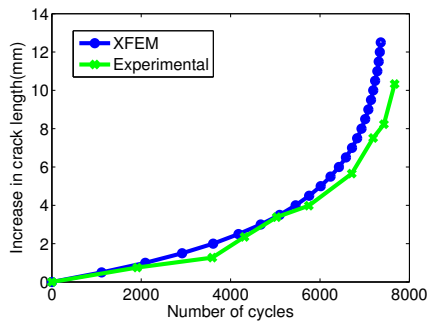
(a) Fatigue life digram for the straight edge cracked specimen
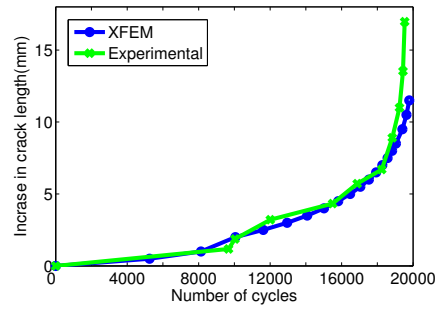
(b) Fatigue life digram for the edge slant cracked specimen
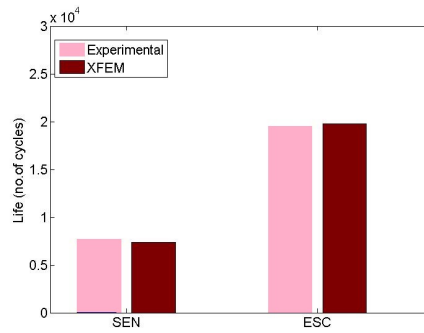
(c) Fatigue life comparison

Figure 3.4: Life diagrams for the edge cracks

Table 3.4: Life

Specimen Type	Experimental	XFEM	Percentage error
SEN	7670	7360	-4%
ESC	19533	19790	+1%

3.6 Conclusion

Using triggering controller the images are taken in regular interval of cycles without stopping loading cycle. We observed that down time for measuring crack can be avoided if use DIC for measuring crack length.

The method was applied to simulate the fatigue life of a rectangular plate in the presence of mode 1 and mixed mode crack under constant amplitude cyclic loading. The results obtained by XFEM were compared with experimental results. These simulations show that the life diagram obtained by XFEM were found in good agreement with experimental solutions. The life of the SEN and ESC specimen shows an error of 4% and -1% percentage respectively. The closely matched experimental and numerical data shows that XFEM is very useful for estimation of fatigue life.

It is also found that the presence of mixed mode crack significantly affect the fatigue life of the materials. Even though we used same crack length, 45° inclination, increased fatigue life by 154% compared with straight crack. The inclined crack is mixed mode problem in which the crack driving force is much less than driving force in the straight crack problems.

Chapter 4

XFEM Modeling of Crack Propagation of Edge Cracked Aluminium Panel

4.1 Introduction

Modeling of moving discontinuities such as propagating crack at using conventional finite element method is highly erroneous in nature. By using XFEM, the entire crack can be represented independently of the mesh, and so remeshing is not necessary to model crack growth. In this work we are modeling the crack growth of aluminum panel using ABAQUS 6.9 which has inbuilt XFEM module in it. We modeled two edge crack geometry such as the straight and inclined crack which represent mode 1 and mixed mode crack respectively. If we know the crack propagation path of a specimen we can redesign the component to get better life.

4.2 Modeling and Simulation

The XFEM capability in ABAQUS6.9 is used to model edge cracked specimens. While using XFEM it is not necessary to model a crack tip singularity or its direction of crack growth. In ABAQUS crack in the form of a wire or area can be define as an enriched zone.
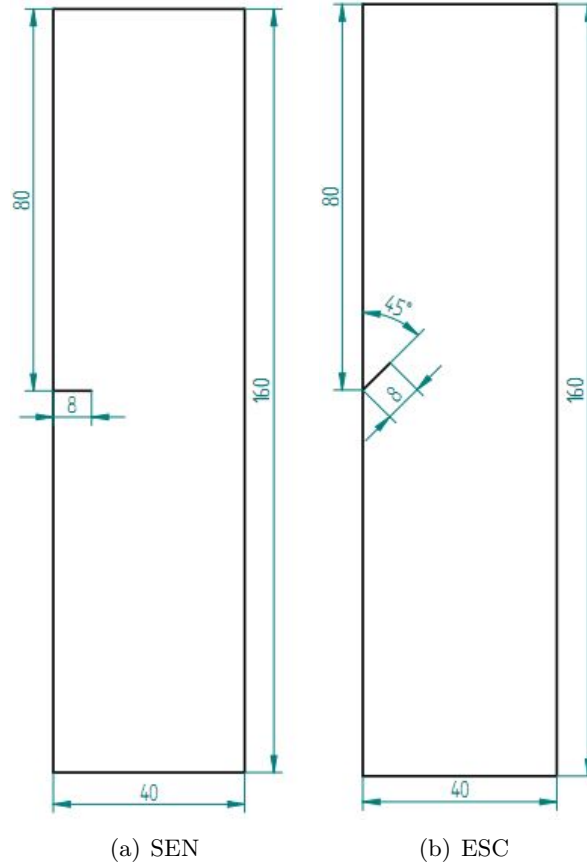
(a) SEN   (b) ESC

Figure 4.1: Model Geometries

Wire and area are used to create crack in 2-D and 3-D problems respectively. In this work we are using 3-D models. Crack is created as an area (3-D shell), then it is assembled to the uncracked plate geometry. In the interaction module, we can define the shell as XFEM crack so that enrichment can be done accordingly. We studied the crack propagation of the straight and inclined edge crack which represent mode 1 and mixed mode crack respectively. The dimension are taken according to ASTM standards [31] as shown in Fig. 4.1

Panels are modeled with elastic plastic models. The properties of AL 6061-T6 from the [35] is used for modeling. The values are given in the Table 4.1

For this study, as mentioned in [35], the maximum principal stress criteria was chosen for the damage criteria ('Maxps Damage' in ABAQUS). The bottom stress in Table 4.2 was used for the maximum principal stress. Damage evolution was based on an energy criteria equivalent to the strain energy release rate, G_1. The damage energy was calculated

Table 4.1: Material Properties of AL 6061-T6

Property	Value
Ultimate Tensile Strength, MPa	317
Young's Modulus, GPa	66.3
Strain at Ultimate Failure	13
Poisson's ratio	0.33

Table 4.2: True Plastic Stress versus True Strain of AL 6061-T6

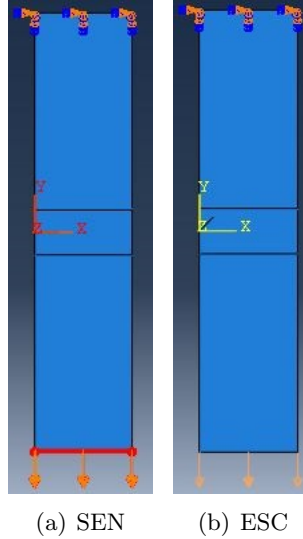| True Plastic stress	True Strain
111.0	0.0000
112.6	0.0019
113.6	0.0038
116.1	0.0067
116.9	0.0086
118.7	0.0135
120.7	0.0183
122.5	0.0231
124.6	0.0279
127.5	0.0326
130.0	0.0421
133.3	0.0514
136.1	0.0607
139.3	0.0699
141.8	0.0790
144.4	0.0881
146.3	0.0971

(a) SEN   (b) ESC

Figure 4.2: Boundary conditions and Load

assuming $G_1 = \frac{K_{1c}^2}{E}$ or 24.2 kN/m. The sub-option for viscosity coefficient was used with a value of 1.e-6.

It is very difficult to get a converged solution for the crack propagation problems. To get a converged solution we need to adjust time step in the step module. The regular meshing can be used for modeling crack using XFEM. To simulate MTS machine in displacement control mode, top end of the specimen is held fixed and on the bottom side a gradual displacement of 10 mm/s is applied as shown in Fig. 4.2

4.3 Results and Discussions

In this work, we have simulated simple geometry like SEN and ESC only. The crack propagation of ESC and SEN panel is shown in Figs. 4.3 and 4.4 respectively. The crack propagation direction matches with the experimental crack.

In this work we used the material properties from the reference [35]. For finding the elastic and plastic properties of a material it is advised to use Ramberg Osgood algorithm which is used to find the Young's modulus, yield stress and other properties from the load displacement data. If we know the yield stress, the plastic properties can be taken from the stress strain data which is beyond yield point in the x axis.
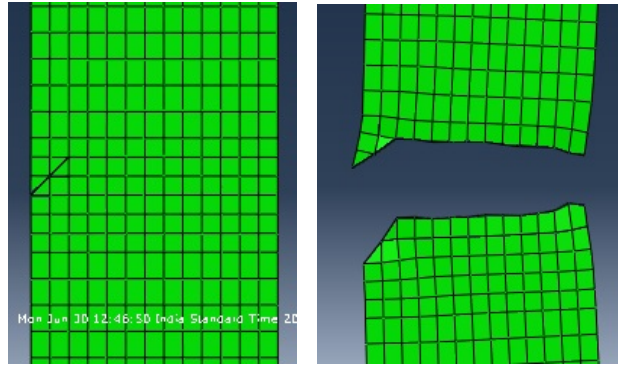
(a) Initial Crack   (b) Final Rupture

Figure 4.3: Crack Growth of ESC
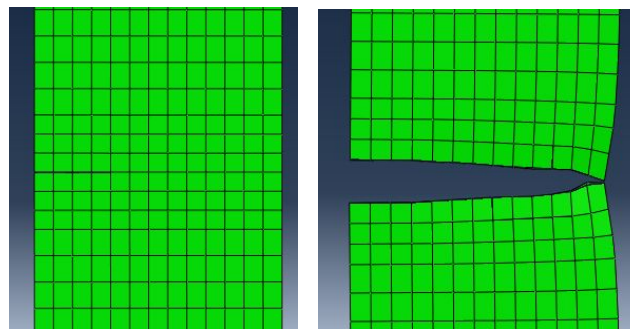
(a) Initial Crack   (b) Final Rupture

Figure 4.4: Crack Growth of SEN

Crack propagation is simulated using XFEM. It is very difficult to get a converged solution. While modeling crack propagation using ABAQUS XFEM, no of increments goes above 5, which is the default maximum number of increments. To avoid this problem we increased the number of increments to 20 in general solution controls. To get the convergence easily we also changed the analysis type from continuous to discontinuous analysis in solution control menu. Then we got converged solution very easily.

4.4 Conclusion

In traditional FEM, we need to give crack propagation direction. But XFEM crack can propagate any direction through the notion of partition of unity. In traditional FEM, it is necessary that the elements should be aligned with crack. But in the case of XFEM the crack can be placed in the uncracked domain independent of meshing.

Crack propagation analysis of SEN and ESC model has been done. The crack is found to be growing through the elements. Without using XFEM it is not possible. So the mesh is need not to be very fine as we do in crack growth problem using cohesive zone modeling. In cohesive zone modeling, crack never grows through the crack

Moreover the crack propagation path matches with actual propagation path. The results show that XFEM is an effective tool for crack propagation analysis.

Chapter 5

Conclusion and Future Scope

From this work it is evident that XFEM is valuable tool for modeling fracture problems. We have successfully done XFEM analysis of following problem.

- Static analysis

- Fatigue life analysis

- Crack propagation modelling

As explained in the Sec. 2.5, SIFs agreeing reasonably with the reference value. But T-stress have a considerable variation from the reference value. If we use a multiparmeter equation which represent both elastic and plastic zone displacement, we will get a better solution.

The fatigue life estimation using XFEM is found to be effective for simple geometries such as SEN and ESC as explained in Sec. 3.6. In industries such as aerospace industries, many components are subjected to fatigue loading. Fuselage is an example for the component which is subjected to fatigue loading. This work can be taken as a benchmark problem and studies can be extended to more complex geometries such as airplane fuselage and adhesively patched metal plates.

The crack propagation using XFEM is found to be effective for simple geometries such as SEN and ESC as explained in Sec. 4.4. This work can be extended to study the failure loads and failure directions for other materials and geometries. Due to increased use of container

tankers and pressurized gas pipe lines, the failure analysis has an increased demand. These problems an be easily analyzed using XFEM. In industries, we can find out many more application for simulation of crack propagation.

References

[1] S. Yoneyama, T. Ogawa, and Y. Kobayashi. Evaluating mixed-mode stress intensity factors from full-field displacement fields obtained by optical methods. *Engineering fracture mechanics* 74, (2007) 1399–1412.

[2] V. Veerkar. A study on experimental determination of mixed mode SIF's using digital photoelasticity and DIC 2012.

[3] T. L. Anderson. Fracture mechanics: fundamentals and applications. CRC press, 2005.

[4] V. Watwood Jr. The finite element method for prediction of crack behavior. *Nuclear Engineering and Design* 11, (1970) 323–332.

[5] T. Nakamura and D. Parks. Antisymmetrical 3-D stress field near the crack front of a thin elastic plate. *International Journal of Solids and Structures* 25, (1989) 1411–1426.

[6] J. Yates, M. Zanganeh, and Y. Tai. Quantifying crack tip displacement fields with DIC. *Engineering Fracture Mechanics* 77, (2010) 2063–2076.

[7] J. M. Melenk and I. Babuška. The partition of unity finite element method: basic theory and applications. *Computer methods in applied mechanics and engineering* 139, (1996) 289–314.

[8] J. Dolbow and T. Belytschko. A finite element method for crack growth without remeshing. *Int. J. Numer. Meth. Engng* 46, (1999) 131–150.

[9] N. Sukumar, D. Chopp, and B. Moran. Extended finite element method and fast marching method for three-dimensional fatigue crack propagation. *Engineering Fracture Mechanics* 70, (2003) 29–48.

[10] P. Kumar. Elements of fracture mechanics. Tata McGraw-Hill, 2008.

[11] Y. Murukami. Stress Intensity Factor Handbook. Oxford, 1987.

[12] J. R. Rice. Limitations to the small scale yielding approximation for crack tip plasticity. *Journal of the Mechanics and Physics of Solids* 22, (1974) 17–26.

[13] B. Cotterell and J. Rice. Slightly curved or kinked cracks. *International Journal of Fracture* 16, (1980) 155–169.

[14] K. Ramesh, S. Gupta, and A. A. Kelkar. Evaluation of stress field parameters in fracture mechanics by photoelasticityrevisited. *Engineering Fracture Mechanics* 56, (1997) 25–45.

[15] S. McNeill, W. Peters, and M. Sutton. Estimation of stress intensity factor by digital image correlation. *Engineering fracture mechanics* 28, (1987) 101–112.

[16] M. Sutton, J. Turner, Y. Chao, H. Bruck, and T. Chae. Experimental investigations of three-dimensional effects near a crack tip using computer vision. *International journal of fracture* 53, (1992) 201–228.

[17] G. Han, M. Sutton, and Y. Chao. A study of stationary crack-tip deformation fields in thin sheets by computer vision. *Experimental Mechanics* 34, (1994) 125–140.

[18] S. Yoneyama, Y. Morimoto, and M. Takashi. Automatic Evaluation of Mixed-mode Stress Intensity Factors Utilizing Digital Image Correlation. *Strain* 42, (2006) 21–29.

[19] G. P. Mogadpalli and V. Parameswaran. Determination of stress intensity factor for cracks in orthotropic composite materials using digital image correlation. *Strain* 44, (2008) 446–452.

[20] A. Mehdi-Soozani, I. Miskioglu, C. Burger, and T. Rudolphi. Stress intensity factors for interacting cracks. *Engineering fracture mechanics* 27, (1987) 345–359.

[21] F. Erdogan and G. Sih. On the crack extension in plates under plane loading and transverse shear. *Journal of basic engineering* 85, (1963) 519–525.

[22] G. C. Sih. Strain-energy-density factor applied to mixed mode crack problems. *International Journal of fracture* 10, (1974) 305–321.

[23] G. C. Sih. Mechanics of fracture initiation and propagation. Springer, 1991.

[24] P. Theocaris and N. Andrianopoulos. The T-criterion applied to ductile fracture. *International Journal of Fracture* 20, (1982) R125–R130.

[25] C. Li. Vector CTD criterion applied to mixed mode fatigue crack growth. *Fatigue & Fracture of Engineering Materials & Structures* 12, (1989) 59–65.

[26] X. Wu and X. Li. Analysis and modification of fracture criteria for mixed-mode crack. *Engineering fracture mechanics* 34, (1989) 55–64.

[27] A. Chambers, T. Hyde, and J. Webster. Mixed mode fatigue crack growth at 550 C under plane stress conditions in Jethete M152. *Engineering Fracture Mechanics* 39, (1991) 603–619.

[28] E. E. Gdoutos. Problems of mixed mode crack propagation. D. Reidel Publishing Co., Hingham, MA, 1984.

[29] A. Abdel Mageed and R. Pandey. Fatigue crack closure in kinked cracks and path of crack propagation. *International Journal of Fracture* 44, (1990) R39–R42.

[30] K. Tanaka. Fatigue crack propagation from a crack inclined to the cyclic tensile axis. *Engineering Fracture Mechanics* 6, (1974) 493–507.

[31] Standard Test Method for Measurement of Fatigue Crack Growth Rates 2011.

[32] A. K. Soh and L. C. Bian. Mixed mode fatigue crack growth criteria. *International Journal of Fatigue* 23, (2001) 427–439.

[33] L. Borrego, F. Antunes, J. Costa, and J. Ferreira. Mixed-mode fatigue crack growth behaviour in aluminium alloy. *International journal of fatigue* 28, (2006) 618–626.

[34] I. Singh, B. Mishra, S. Bhattacharya, and R. Patil. The numerical simulation of fatigue crack growth using extended finite element method. *International Journal of Fatigue* 36, (2012) 109–119.

[35] J. C. Lyonel Reinhardt. XFEM Modeling of Mixed-Mode Cracks in Thin Aluminum Panels. *SIMULIA Customer Conference* .

[36] K. M. Saranath and M. Ramji. Fatigue crack growth modeling of an interacting crack system using finite element analysis 2013.